Journal of Alloys and Compounds 512 (2012) 264–269

Contents lists available at SciVerse ScienceDirect

Journal of Alloys and Compounds

journal homepage: www.elsevier.com/locate/jallcom

Citric based sol–gel synthesis and luminescence characteristics of $CaLa_2ZnO_5:Eu^{3+}$ phosphors for blue LED excited white LEDs

Vengala Rao Bandi[a], Bhaskar Kumar Grandhe[a], Kiwan Jang[a,*], Ho-Sueb Lee[a], Dong-Soo Shin[b], Soung-Soo Yi[c], Jung-Hyun Jeong[d]

[a] Department of Physics, Changwon National University, Changwon 641-773, Republic of Korea
[b] Department of Chemistry, Changwon National University, Changwon, Republic of Korea
[c] Department of Photonics, Silla University, Busan, Republic of Korea
[d] Department of Physics, Pukyong National University, Busan, Republic of Korea

ARTICLE INFO

Article history:
Received 11 July 2011
Received in revised form
26 September 2011
Accepted 28 September 2011
Available online 4 October 2011

Keywords:
Oxide materials
Sol–gel processes
Optical properties

ABSTRACT

A novel class of orange–red phosphors namely $CaLa_2ZnO_5$ (CLZ) doped with Eu^{3+} ions were prepared by adopting citrate based sol–gel method. Those were thoroughly characterized by means of XRD, SEM, Tg-DTA, photoluminescent (PL) spectral profiles. PL studies reveal that its emission intensity strongly depends on sintering temperature as well as the dopant ion (Eu^{3+}) concentration. Eu^{3+} ion doped $CaLa_2ZnO_5$ phosphor has a strong excitation at 468 nm, which correspond to the popular emission line from a GaN based blue light-emitting diode (LED) chip. The influence of the preparation method on the luminescence property was studied by comparing the emission performance of phosphors prepared by sol–gel and solid-state reaction methods along with a commercial red phosphor $Y_2O_2S:Eu^{3+}$. Thus, the intense red emission ($^5D_0 \rightarrow {}^7F_2$) of the Eu^{3+} doped CLZ phosphors under blue excitation suggests them to be a potential candidate for the production of white light by blue LEDs.

© 2011 Elsevier B.V. All rights reserved.

1. Introduction

White light-emitting diodes (WLEDs), as an emerging solid state lighting (SSL) source, offers benefits in terms of reliability, energy saving, maintenance and positive environment effects and stands a real chance of replacing the traditional light sources such as incandescent and fluorescent lamps [1–3]. Now a days most of the commercial solid-state devices are using nearly monochromatic blue emission from GaN based LEDs to excite yellow–green emission from Ce^{3+}-doped yttrium aluminum garnet (YAG:Ce) phosphors. These devices produce light in the blue to yellow portion of the visible spectrum, which means that orange or red objects appear dim and colorless under this lighting. WLEDs with YAG:Ce phosphors have low color-rendering index and high correlated color temperature because of its weak emission intensity in the red spectral region. Thus to improve their white light quality, these devices require potential red emitting phosphors that can be excited by blue LEDs [4–6]. Most of the red phosphors are doped with Eu^{2+} ions whose emissions are generally due to parity-allowed 5d–4f transitions. The 5d orbitals are spatially diffused and their energy levels strongly depend on the local crystal field of the surrounding ions in the lattice [7,8]. This leads to the emission band broadening because of the differences in the atomic environments (inhomogeneous broadening) and phonon coupling (homogeneous broadening). An undesired consequence of this broad emission is the deep-red emission, which is insensitive to human eye. The absorption bands are also broad, which not only enables excitations in near-UV to visible LEDs, but also triggers needless absorption of green or yellow emission from other phosphors in the blends. For these reasons, we have focused on narrow band red-emitting phosphors with blue region absorption for solid state lighting (SSL) applications. In order to achieve high luminous output, the emission band should possess the smaller full width at half-maximum (FWHM) values. Conventional phosphors used in Hg based fluorescent lamps excited at 254 nm UV light are not ideal for SSL because they have poor absorption for LED light (in the near UV or blue region) [9]. The presently used red and green phosphors for blue LEDs are $SrY_2S_4:Eu^{2+}$ and $SrGa_2S_4:Eu^{2+}$ respectively [10,11]. However, these sulfide-based phosphors are thermally unstable and very much sensitive to moisture. Their luminescence degrades significantly under ambient atmosphere without a protective coating layer. Besides, they are chemically unstable due to releasing of sulfide gas and also the lifetime of these materials are low under UV or blue light irradiation [11,12]. Therefore, exploring a stable, inorganic rare-earth based red phosphor with high absorption in the blue region is an essential and significant research task.

* Corresponding author. Tel.: +82 55 213 3425; fax: +82 55 267 0263.
E-mail address: kwjang@changwon.ac.kr (K. Jang).

0925-8388/$ – see front matter © 2011 Elsevier B.V. All rights reserved.
doi:10.1016/j.jallcom.2011.09.078

To identify the novel efficient red phosphors for WLEDs, the choice of the activator ions is another key factor. Among all the activators, the optical properties of the Eu^{3+} ion doped materials are significant because it possesses proper chromaticity coordinates. The lowest excited level ($^5D_0$) of the $4f^6$ configuration is situated below the $4f^55d$ configuration for Eu^{3+}. When Eu^{3+} ions occupy the lattice sites noncentrosymmetry lattice centers, it is favorable to improve the color purity of the red phosphor due to their intense $^5D_0 \rightarrow {}^7F_2$ emission in the red spectral region. Moreover, most of the Eu^{3+} doped phosphors possess intense absorption in the UV to blue region [13,14].

To obtain red luminescent materials with high quantum efficiencies, the nature of host matrix is worthy to be taken into account. The ternary oxides XY_2ZO_5 (X = Ba, Y = rare-earth, Z = Cu, Zn) are receiving much attention because of their very interesting structural, physical and chemical properties and additionally they exhibit special magnetic, optical and superconducting properties [15–17]. Owing to these reasons, in the present investigation we have chosen $CaLa_2ZnO_5$ as the host matrix for doping Eu^{3+} ions. Phosphors that are synthesized by the conventional solid state reaction method usually require a relatively long-term sintering at the higher temperature consuming huge energy, which is also contradiction to the motto of energy saving characteristics of SSL. The grinding process is necessary to prepare phosphors by solid-state reaction method. However, it generally degrades luminescent efficiencies due to the introduction of surface defects that act as non-radiative recombination sites. Therefore, phosphor synthesis techniques that can overcome the disadvantages of high-temperature solid-state reaction method are of great importance [18,19]. Here, we have adopted citrate based sol–gel method which is a simple, economical and yet an effective method for preparing luminescent materials, because it offers many advantages like high purity, relatively lower sintering temperature and in a much shorter sintering time. In the present paper we report our investigations on the structural and photoluminescence properties of Eu^{3+} doped CLZ phosphors prepared by adopting citrate based sol–gel method. As far as our knowledge is concerned, this novel piece of work has not been reported earlier on the CLZ host matrix.

2. Experimental

A series of red phosphors namely $CaLa_{2-x}Eu_xZnO_5$ (x = 0.001, 0.005, 0.01, 0.05, 0.1 and 0.12) were synthesized by the citrate sol–gel method (SG) using $CaCO_3$, La_2O_3, ZnO, Eu_2O_3 as the starting materials. Stoichiometric amounts of corresponding oxides were dissolved in HNO_3 (AR grade) under vigorous stirring. De-ionized water and ethanol was then added to the above solution in the volumetric ratio of 1:4. Later, certain quantity of citric acid (AR grade) was added to the above solution as a chelating agent such that the molar ratio of total metal cations to citric acid should be in the ratio of 1:3. Finally, the pH of the resultant solution was brought down to 7 by adding the suitable amount of NH_3 aqueous solution. Highly transparent solution was obtained after stirring it for a few minutes. The resulted transparent solution was heated at 80 °C and stirring it for while yielded a light-brown gel. The gel thus obtained was collected and oven-dried at 120 °C for 12 h in order to obtain the CLZ phosphor precursor. This precursor was then heated at 400 °C for 3 h followed by sintering at required temperatures from 750 °C to 1150 °C for 5 h to obtain the phosphor samples. Apart from this, 10 mol% Eu^{3+}-doped CLZ phosphor was also prepared by a solid-state reaction method (SSR) a comparison purpose. Highly pure and reagent grade chemicals, such as $CaCO_3$, La_2O_3, ZnO and Eu_2O_3 were used as starting materials. Required chemicals were weighed based on its stiochiometric composition and grinded in an agate mortar with acetone in order to obtain a homogeneous chemical mixture. This chemical mixture was then transferred to an alumina crucible and heated in an electrical furnace from room temperature to 1100 °C. It was sintered at this high temperature for about 5 h with an intermediate grinding.

The structure of these samples were investigated by employing a Philips X'pert, MPD 3040 X-ray diffractometer with Cu Kα radiation (λ = 1.5406 Å) at 40 kV and 30 mA. Thermogravimetry (TG) and differential thermal analysis (DTA) of the CLZ phosphor precursor was studied on a TA 5000/SDT 2960 DSC Q10 in N_2 atmosphere with an heating rate of 10 °C/min. Morphological features of the prepared phosphors were observed by field emission scanning electron microscope (Tescan, MIRA II LMH) with a working distance of 5 mm, 20 k× magnification and 20 kV operating voltage. The photoluminescent excitation and emission spectra of these phosphors were recorded on Shimadzu, RF-5301PC spectrofluorophotometer.

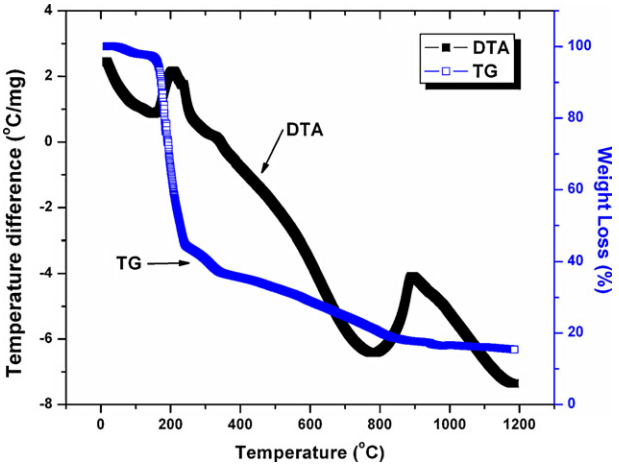

Fig. 1. Tg-DTA profiles of CLZ phosphor precursor.

3. Results and discussion

The Tg-DTA profile of the CLZ phosphor precursor was shown in Fig. 1. The total weight loss occurred can be roughly divided into four stages: (1) from 100 °C to 180 °C, 3% weight loss due to the evaporation of the water and ethanol accompanied by the endothermic peak at 175 °C; (2) from 180 °C to 265 °C, about 54% weight loss due to the burning of the citric acid ligand and the decomposition of metal nitric, which was accompanied by the two exothermic peaks at 209 and 240 °C; (3) 23% weight loss from 265 °C to 800 °C arising from the further combustion of the citric acid as well as the de-hydroxylation and oxidation of the decomposed fragment, which was accompanied by the two exothermic peaks around 330 °C and 570 °C; (4) in the final stage only 5% of weight loss from 800 °C to 1200 °C, which aroused due to decomposition of any other organic residue. The exothermic peak observed at 890 °C represents the crystallization process of CLZ phosphor. The obtained results are in good agreement with the earlier reported results [20,21].

Fig. 2a depicts the excitation spectrum of 10 mol% Eu^{3+}-doped CLZ phosphor sintered at 1100 °C and monitored with 627 nm as the emission wavelength. We noticed sharp excitation bands corresponding to the characteristic f–f transitions of Eu^{3+} ions within its $4f^6$ configuration. These bands were aroused due its transition

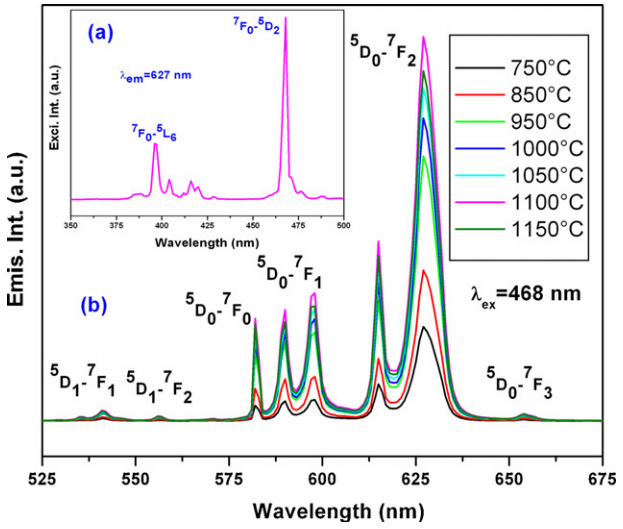

Fig. 2. (a) Excitation; (b) emission spectra of CLZ:Eu^{3+} (10 mol%) phosphors at various temperatures.

from the ground state $^7F_0$ to $^5G_{2,4,}$ $^5L_6$, $^5D_3$ and $^5D_2$ at 386, 396, 415 and 468 nm respectively. Among all the excitation bands observed, the intense excitation band at 468 nm ($^7F_0 \rightarrow {}^5D_2$) was suitable to make use of the emission light generated by the blue LED chip. No remarkable difference was found with regard to the location of the Eu^{3+} emission lines in the above phosphor excluding their relative intensities when the excitation wavelengths are 396 nm and 468 nm. For this reason, emission spectra of 10 mol% Eu^{3+}-doped CLZ phosphors sintered at various temperatures and excited with 468 nm are alone displayed in Fig. 2b. It consists of lines in the orange and red spectral region exhibiting the characteristic f-f transitions of Eu^{3+}. They are $^5D_1 \rightarrow {}^7F_1$ (541 nm), $^5D_1 \rightarrow {}^7F_2$ (557 nm), $^5D_0 \rightarrow {}^7F_0$ (582 nm), $^5D_0 \rightarrow {}^7F_1$ (590 and 598 nm), $^5D_0 \rightarrow {}^7F_2$ (615 and 627 nm) and $^5D_0 \rightarrow {}^7F_3$ (654 nm) respectively [22–24]. It can be seen from this figure that the spectra is dominated by the prominent band at 627 nm due to the $^5D_0 \rightarrow {}^7F_2$ transition. It is well known that the $^5D_0 \rightarrow {}^7F_2$ emission belongs to hypersensitive transition with $\Delta J = 2$, which is strongly influenced by the outside surroundings. When the Eu^{3+} is located at a low symmetry local site, this emission transition is often dominated in their emission spectra. The splitting of $^5D_0$–$^7F_1$ emission peak might be due to spin orbital interactions of Eu^{3+}. It was also observed that, with the increasing of sintering temperature, the emission intensity enhanced significantly and reaching a maximum value for 1100 °C. This phenomenon occurs due to the reduction of non-radiative recombination effects, quenching sites, and surface defects trapped by increased crystallinity and decreased defects in the crystal. The better crystallinity of the $CaLa_2ZnO_5$:Eu^{3+} phosphors sintered at 1100 °C was the main reason for its superior emission when compared to the other samples. It is also in agreement with the results of the XRD analysis, as optimum crystallinity was obtained at 1100 °C. When sintering temperature (1100 °C) is increased further, the emission intensity is decreasing significantly as a result of the agglomeration caused by specific sintering between the grains at a higher sintering temperature. Also, energy transfer to neighboring ions will be quenched by the grain boundaries and defects that are introduced by further sintering of the sample. No distinct variations in the shape and position of emission spectral features were noticed when the sintering temperature was varied in a wide range. These results indicate that the order of the environment surrounding the Eu^{3+} ions have a great impact on the PL emission intensity.

The doping concentration of luminescent center is one of the important factor that influence the efficiency of a phosphor. Therefore, it is necessary to identify the optimum doping concentration. The integrated emission intensities of $^5D_0 \rightarrow {}^7F_J$ ($J = 0$–3) transitions of CLZ phosphors doped with various Eu^{3+} ion concentrations were calculated, and the dependence of the emission intensity from the $^5D_0 \rightarrow {}^7F_2$ hypersensitive transition of Eu^{3+} ion doped CLZ phosphor is shown in Fig. 3a. The intensity enhances with the increase of doping concentration and reaches a maximum at 10 mol% Eu^{3+} ion doping concentration. For 12 mol% Eu^{3+} ion doping concentration, the intensity of the $^5D_0 \rightarrow {}^7F_2$ transition was decreased by a nominal value only. The concentration quenching here occurs at a higher concentration. Blasse et al. proposed that the quenching mechanism is associated with the exchange interaction and it ultimately quenches the emission from the $^5D_0$ level of the Eu^{3+} ion [25]. Recently, it was reported that the ratio between the integrated intensity of the transitions $^5D_0 \rightarrow {}^7F_2$ and the $^5D_0 \rightarrow {}^7F_1$, represented as I_{0-2}/I_{0-1}, as a local crystal field probe to measure the nature of the local cation surroundings. That is to say, this intensity ratio supplies a new avenue to estimate the degree of distortion from the inversion symmetry of the Eu^{3+} ion local environment. We have plotted these ratios with respect to the amount of Eu^{3+} (x) used in the samples and is shown in Fig. 3b. For the sintering temperature of 1100 °C, the ratio of integrated intensity I_{0-2}/I_{0-1} was found to increase with increasing Eu^{3+} ion concentration [26].

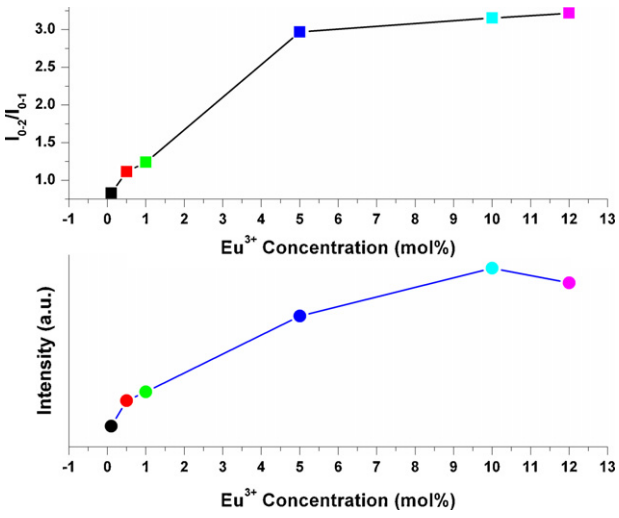

Fig. 3. (a) Red emission intensity ($^5D_0 \rightarrow {}^7F_2$); (b) intensity ratio I_{0-2}/I_{0-1} of Eu^{3+} as a function of its doping concentration in CLZ:Eu^{3+} phosphors sintered at 1100 °C excited by 468 nm.

This implies that the local environment of activator Eu^{3+} ion was more distorted with an increased amount of its concentration in the present series of phosphors. The relative intensity of $^5D_0 \rightarrow {}^7F_J$ multiplet emission is also an important factor that determines the chromaticity or saturation of red color and in general, the larger the magnitude of (($^5D_0 \rightarrow {}^7F_2$)/($^5D_0 \rightarrow {}^7F_1$)) (R/O), the closer to the optimal value of the color chromaticity [27,28]. Eu^{3+} ion is very much sensitive to its surrounding environment. The effect of the crystal field will cause shifts and splitting of the crystal field levels. From the crystal structure considerations of $CaLa_2ZnO_5$ host matrix, the REO_8 polyhedra are distorted with distortions being of both even and odd parity. In terms of even parity, the crystal field expansion will cause splitting in the electronic energy levels of the corresponding RE^{3+} ions, while odd parity leads to the enhancement of dipole transitions between the RE^{3+} ion multiplets [29,30]. The complicated emission profiles of Eu^{3+} doped CLZ phosphors involving large scale $^5D_{0,1} \rightarrow {}^7F_J$ ($J = 0$, 1, 2, 3) transitions can be ultimately ascribed to the odd parity distortions of the environment around the Eu^{3+} ions.

The typical PL spectra of the CLZ:Eu^{3+} phosphor with that of standard YAG:Ce^{3+} has been shown in Fig. 4. The YAG:Ce^{3+} phosphor can be effectively excited by the 470 nm blue light and emits strong yellow emission at 540 nm. However, YAG:Ce^{3+} does not almost absorb n-UV (≈400 nm), and its emission is silent under the 400 nm light irradiation. The white light realized by the combination with a blue LED exhibit a poor color rendering index due to the lack of red color component. In the present investigation, the emission of CLZ:Eu^{3+} phosphor occurs at a fairly longer wavelength in the orange and red spectral region under the excitation wavelength of 468 nm, which perfectly matches with the emission wavelength of blue LEDs. These results suggest that the CLZ:Eu^{3+} phosphor could be used as an efficient orange–red emitting phosphor in WLEDs. The Commission International del'Eclairage (CIE) chromaticity coordinates of 10 mol% Eu^{3+}-doped CLZ phosphor are shown in an inset Fig. 4. The chromaticity coordinates of CLZ:Eu^{3+} phosphors are (0.658, 0.341) for the optimum Eu^{3+} ion doping concentration. The characteristic index shows that the red emitting CLZ:Eu^{3+} phosphors have higher color saturation. Furthermore, based on its excitation spectrum we can say that the CLZ:Eu^{3+} phosphors can efficiently absorb the emission of blue GaN LED and it can also emit strong red color. Thus, the prepared CLZ phosphor can be used to compensate the red color deficiency of YAG:Ce^{3+} based white LEDs or to produce white light by combining with

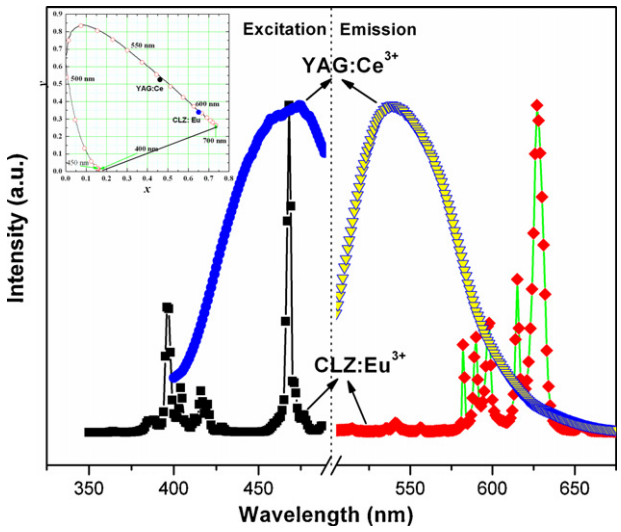

Fig. 4. Typical photoluminescence spectra of CLZ:Eu^{3+} and YAG:Ce^{3+}. Inset shows CIE chromaticity coordinates of CLZ:Eu^{3+}, Y_2O_2S:Eu^{3+} and YAG:Ce^{3+}.

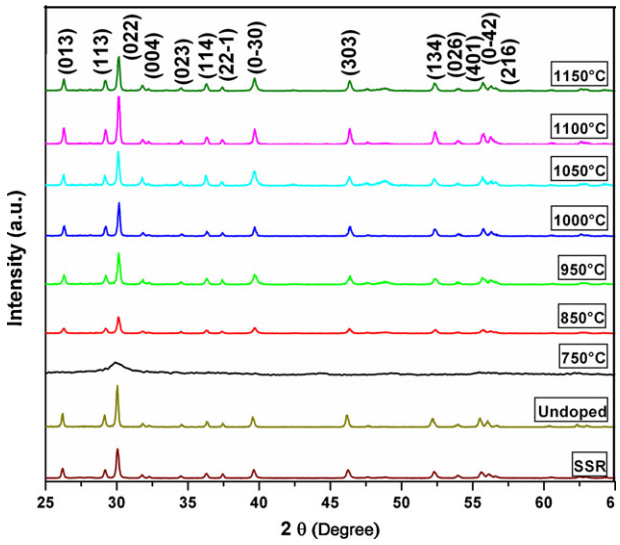

Fig. 6. XRD patterns of CLZ:Eu^{3+} (10 mol%) phosphor prepared by SSR method at 1100 °C along with un-doped CLZ and CLZ:Eu^{3+} (10 mol%) phosphors prepared by sol–gel method at different temperatures.

a blue chip and another green phosphor. Therefore, CLZ:Eu^{3+} red phosphor might be a potential candidate for fabricating white LEDs.

Fig. 5 shows the emission spectra of CLZ:Eu^{3+} phosphors, which were prepared by the sol–gel and solid state reaction methods and those were compared along with emission performance of commercial red phosphor Y_2O_2S:Eu^{3+} when the excitation wavelength is 468 nm. It can be seen that all the phosphors have displayed similar emission lines but with varying intensities. We also noticed that the emission intensity of the phosphors prepared via the sol–gel based method was much better than that of the phosphors prepared by solid-state reaction process as well as commercial Y_2O_2S:Eu^{3+} phosphor. In the sol–gel process, citric acid acts as a chelating agent and forms a large amount of tiny enclosures that can effectively trap the constituent metal ions. The enhancement in emission intensity was observed, since the citrate based sol–gel method provides a homogeneous environment than the solid-state mixing and besides the uniformity in distribution of Eu^{3+} ions in the CLZ host matrix was also enhanced. The high crystallinity and uniform distribution of Eu^{3+} activators reduce the non-radiative relaxation and results

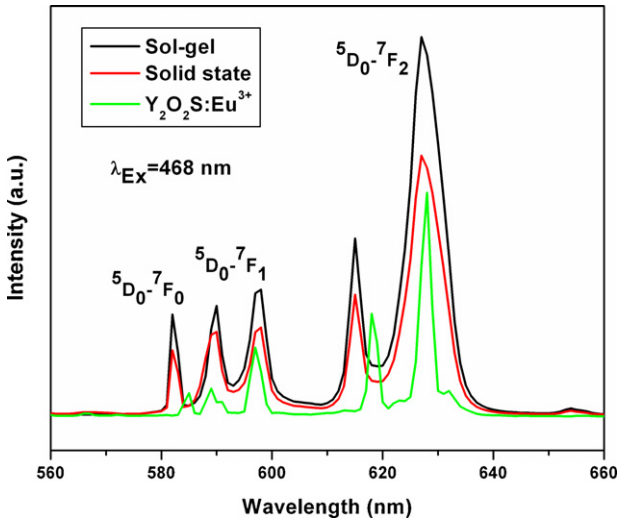

Fig. 5. Comparison of emission intensity of CLZ:Eu^{3+} phosphors prepared by (a) sol–gel; (b) solid state method; (c) Y_2O_2S:Eu^{3+} red phosphor.

in an increase in the emission intensity. Moreover, doping of impurities is easier and effective in SG process than in conventional SSR, since all the starting materials were mixed at the molecular level. So the emission intensity of the sol–gel prepared CLZ phosphor has been enhanced. Thus the citrate based sol–gel method has been confirmed to be a valid and efficient method for the fabrication of the CLZ phosphors.

The XRD patterns of 10 mol% Eu^{3+}-doped CLZ phosphor synthesized by the sol–gel method with different sintering temperatures between 750 °C and 1150 °C were shown in Fig. 6. Besides, in the above figure, we have also presented the XRD patterns of the CLZ phosphor prepared by means of solid state reaction method at 1100 °C for a comparison purpose. Samples sintered at 750 °C did not revealed any diffraction peaks, except a broad band centered at $2\theta = 30°$, which might be due to the formation of an amorphous product or very small crystallites. As the sintering temperature was increased to 950 °C, the XRD pattern displayed peaks that are in close resemblance with the respective host reflections. This result demonstrates that the activator Eu^{3+} ion has been successfully doped into the host lattice. However, in the present investigation the XRD pattern of CLZ:Eu^{3+} does not coincide with the individual oxide systems and also it can be clearly seen that there is no exact correlation between La_2O_3 and CLZ:Eu^{3+}. Based on both the theoretical simulation and XRD analysis by a software namely POWD, we found that the structures of them are tetragonal natured and the corresponding ($h\,k\,l$) values for the obtained diffraction peaks were indexed appropriately. Besides, CLZ crystal structure is similar to that of $BaLa_2ZnO_5$ and $BaNd_2ZnO_5$, which are well agreement with the tetragonal structure [16,17]. Further heat treatment at 1000 °C, 1050 °C and 1100 °C leads to the enhancement in the diffraction peak intensity and reduction in FWHM due to the improvement of crystallinity and grain growth. The above results indicate that optimized CLZ phosphor can be obtained at 1100 °C with 10 mol% of Eu by sol–gel method.

The sintering temperature used here is relatively lower than the conventional solid-state reaction method, confirming the advantage of the adopted sol–gel method. The reasons for the lower crystalline temperature may be attributed to two aspects. Firstly, the sol–gel method provides a molecular level mixing of constituent elements due to the fact that these metal ions are homogeneously dissolved in liquid sate and then chelated as a

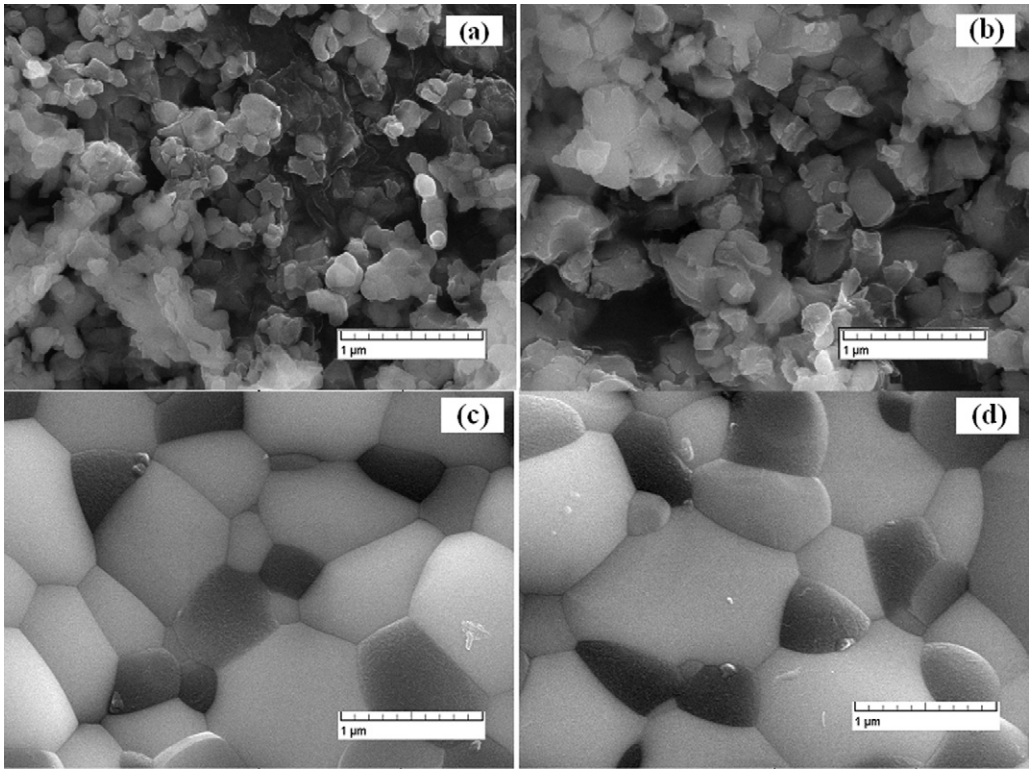

Fig. 7. SEM images of the CLZ:Eu^{3+} (10 mol%) phosphors at (a) 850 °C, (b) 950 °C, (c) 1100 °C and (d) 1150 °C.

metal complex. This reduces the diffusion path for obtaining the desired material and as a consequence needs lower synthesis temperature compared to the conventional solid-state method. Secondly, in the gel thus formed, there exits enormous polymeric content which can act as fuel and NO_{3-} as an oxidant. During the pre-calcination process, the fuel can be ignited at low temperature (about 400 °C) and reaches high temperature in a short period of time, which can possibly accelerate the crystallization process.

Fig. 7 shows the SEM micrographs of 10 mol% Eu^{3+}-doped CLZ samples that were prepared by using sol–gel method and sintered at different temperatures. Most of the particles are irregular in shape and agglomerated. Both the particle size and the extent of the agglomeration are increasing with the increase in sintering temperature. Fig. 7a and b display the images of the sample prepared at 850 and 950 °C, among, most of the particles are smaller than 300 nm in diameter, including some below 100 nm. Fig. 7c and d shows the SEM observation of the CLZ phosphors sintered at 1100 and 1150 °C, which particles are in the range of micro meter in size. It can be seen from Fig. 7b that the grain boundaries of the phosphor samples sintered at 950 °C are not clear due to elongated necks between two grains. We can also observe some pores which are probably due to the release of some gaseous byproducts during its sintering. Therefore, its grain growth might be hindered. As the sintering temperature increases, the necks between grains and the pores disappear along with the conglomeration of smaller grains in to larger grains. Higher sintering temperature enhances higher atomic mobility and causes faster grain growth. Hence, increase in sintering temperature will naturally lead to increase in the particle size [31–33]. It is evident that most of the particles are in micrometer range, which is a suitable size for the fabrication of SSL devices [25]. The XRD patterns also show increased sharpness of diffraction peaks, inferring the growth of crystallite size with increased sintering temperature. The effects of particle size and agglomeration on PL properties are quite significant.

4. Conclusions

In brief, a novel class of orange–red phosphors namely CLZ:Eu^{3+} phosphors were prepared by adopting citrate based sol–gel method. Optimal sintering temperature and activator concentration have been determined to be 1100 °C and 10 mol% respectively. The prepared phosphors showed intense orange–red emissions corresponding to the $^5D_{0,1} \rightarrow {}^7F_J$ transitions of Eu^{3+} with blue excitation of 468 nm, which is very close to the emission wavelength of blue LED. The CIE color coordinates of the 10 mol% Eu^{3+}-doped CLZ phosphor with the strong red emission intensity is closer to the NTSC standard values. Obtained results indicate that CLZ:Eu^{3+} phosphor prepared by sol–gel method is better than those of the phosphors prepared by solid-state reaction method and commercial red phosphor Y_2O_2S:Eu^{3+}. Owing to these encouraging photoluminescence spectral profiles, it can be concluded that the Eu^{3+}-doped CLZ system with a higher doping concentration under the excitation of blue (468 nm) light could be a promising orange–red-emitting phosphor for its application in White LED devices.

Acknowledgements

This work was supported by the Priority Research Centers Program through the National Research Foundation of Korea funded by the Ministry of Education, Science and Technology (NRF-2010-0029634) and also this work was partially supported by the National Research Foundation of Korea funded by the Korean Government (NRF-2010-0023034).

References

[1] S. Yan, Y. Chang, W. Hwang, Y. Chang, M. Yoshimura, C. Hwang, J. Alloys Compd. 509 (2011) 5777–5782.
[2] N. Khan, N. Abas, Renew. Sust. Energy Rev. 15 (2011) 296–309.
[3] C. Lin, R. Liu, J. Phys. Chem. Lett. 2 (2011) 1268–1277.

[4] S. Ye, F. Xiao, Y.X. Pan, Y.Y. Ma, Q.Y. Zhang, Mater. Sci. Eng. R 71 (2010) 1–34.
[5] Y. Chen, J. Wang, X. Zhang, G. Zhang, M. Gong, Q. Su, Sens. Actuators B: Chem. 148 (2010) 259–263.
[6] B.V. Rao, K. Jang, H. Lee, S. Yi, J. Jeong, J. Alloys Compd. 496 (2010) 251–255.
[7] H.A. Hoppe, Angew. Chem. Int. Ed. 48 (2009) 3572–3582.
[8] C.C. Lin, Z.R. Xiao, G. Guo, T. Chan, R. Liu, J. Am. Chem. Soc. 132 (2010) 3020–3028.
[9] X. He, M. Guan, N. Lian, J. Sun, T. Shang, J. Alloys Compd. 492 (2010) 452–455.
[10] L. Li, X. Shen, L. Li, X. Meng, J. Sol–Gel Sci. Technol. 57 (2011) 198–203.
[11] P.F. Smet, I. Moreels, Z. Hens, D. Poelman, Materials 3 (2010) 2834–2883.
[12] M. Thomas, P.P. Rao, S.P.K. Mahesh, L.S. Kumari, P. Koshy, Phys. Status Solidi A 208 (9) (2011) 2170–2175.
[13] H.Y. Jiao, Y.H. Wang, Appl. Phys. B 98 (2010) 423–427.
[14] A. Xie, X. Yuan, F. Wang, Y. Shi, J. Li, L. Liu, Z. Mue, J. Alloys Compd. 501 (2010) 124–129.
[15] G.K. Cruz, H.C. Basso, M.C. Terrile, R.A. Carvalho, J. Lumin. 86 (2000) 155–160.
[16] J.A. Kauduk, W. Wong-Ng, W. Greenwood, J. Dillingham, B.H. Toby, J. Res. Natl. Inst. Stand. Technol. 104 (1999) 147.
[17] A. Kan, H. Ogawa, K. Mori, J. Sugishita, Mater. Res. Bull. 37 (2002) 1509–1518.
[18] Z. Jun, W. Yu-Hua, L. Bi-Tao, L. Ji-Di, Chin. Phys. B 19 (12) (2010) 127809.
[19] B.K. Grandhe, V.R. Bandi, K. Jang, S. Ramaprabhu, S. Yi, J. Jeong, Electron. Mater. Lett. 7 (2) (2011) 161–165.
[20] Q. Meng, J. Lin, L. Fu, S. Wang, Y. Zhou, J. Mater. Chem. 11 (2001) 3382–3386.
[21] M.P. Saradhi, B. Raveau, V. Caignaert, U.V. Varadaraju, J. Solid State Chem. 183 (2010) 485–490.
[22] X. Xiao, B. Yan, Y. Song, Cryst. Growth Des. 29 (2009) 136–144.
[23] V.R. Bandi, Y. Nien, T. Lu, I. Chen, J. Am. Ceram. Soc. 92 (2009) 2953–2956.
[24] V. Venkatramu, M. Giarola, G. Mariotto, S. Enzo, S. Polizzi, C.K. Jayasankar, F. Piccinelli, M. Bettinelli, A. Speghini, Nanotechnology 21 (2010) 175703.
[25] V.R. Bandi, M. Jayasimhadri, J. Jeong, K. Jang, H. Lee, S. Yi, J.H. Jeong, J. Phys. D: Appl. Phys. 43 (2010) 395103.
[26] G.S.R. Raju, H. Jung, J.Y. Park, B.K. Moon, R. Balakrishnaiah, J.H. Jeong, J.H. Kim, Sens. Actuators B: Chem. 146 (2010) 395–402.
[27] F. Du, Y. Nakai, T. Tsuboi, Y. Huang, H.J. Seo, J. Mater. Chem. 21 (2011) 4669.
[28] C. Wu, K. Chen, C. Lee, T. Chen, B. Cheng, Chem. Mater. 19 (2007) 3278.
[29] X. Qi, R. Illingworth, H.G. Gallagher, T.P.J. Han, B. Henderson, J. Cryst. Growth 160 (1–2) (1996) 111–118.
[30] L.S. Kumari, P.P. Rao, M. Thomas, P. Koshy, J. Electrochem. Soc. 156 (8) (2009) P127–P131.
[31] Y. Hsiao, Y. Chang, Y. Chang, Mater. Sci. Eng. B 136 (2007) 129–133.
[32] S.L. Kang, Sintering: Densification, Grain Growth, and Microstructure, first ed., Elsevier Butterworth-Heinemann, Burlington, 2005.
[33] S.P. Khatkar, S. Han, V.B. Taxak, Opt. Mater. 29 (2007) 1362–1366.